Effect of changing hot-wire temperature on SEA Ice Crystal Detector

Fleury, Liam; Nichman, Leonid; Bliankinshtein, Natalia

Laboratory Technical Report (National Research Council Canada. Flight Research Laboratory); no. LTR-FRL-2025-0092, 2025-06-09

Effect of Changing Hot-wire Temperature on SEA Ice Crystal Detector

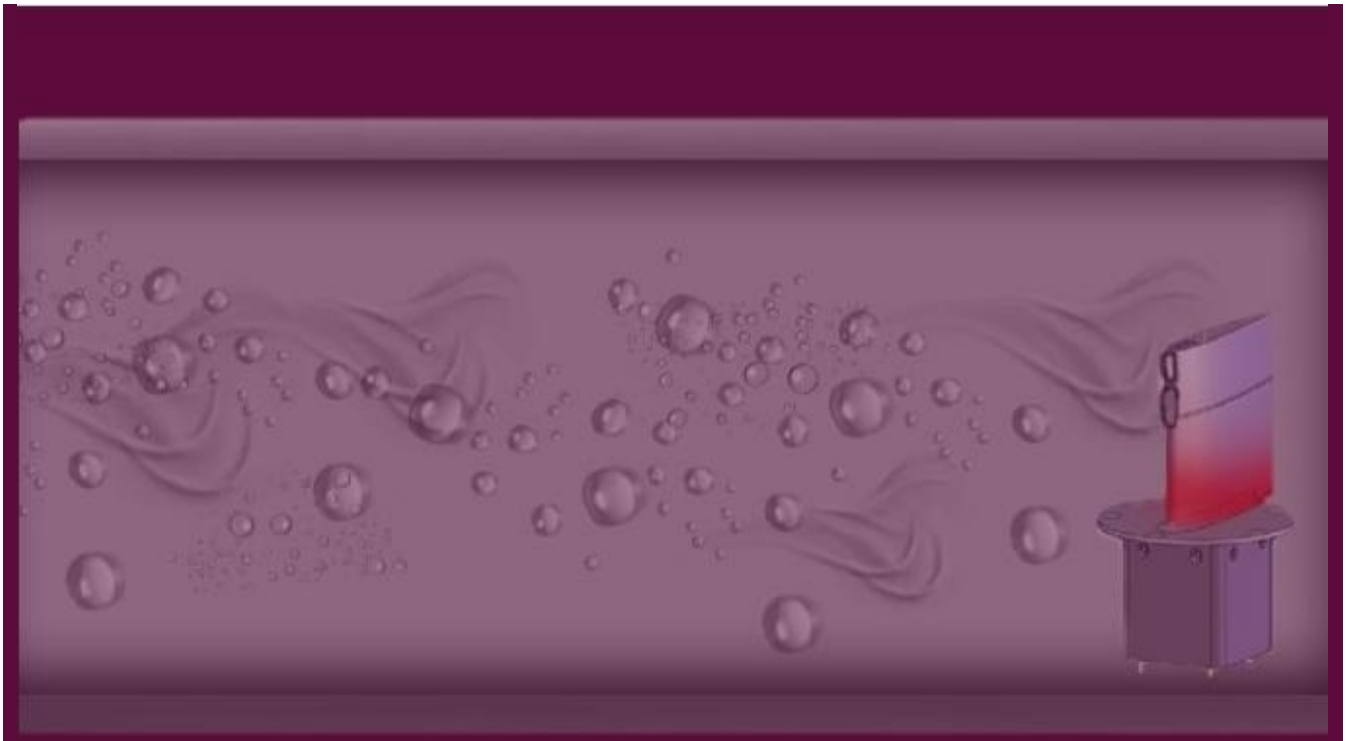

Non-sensitive

Report No: LTR-FRL-2025-0092
June 09, 2025

Liam Fleury

Leonid Nichman

Natalia Bliankinshtein

National Research Council Canada | Conseil national de recherches Canada

Canada

Table of contents

Figure List

Table List

Acronym List

AIWT – Altitude Icing Wind Tunnel

APDC – Aeronautical Product Development and Certification

ICD – Ice Crystal Detector

LWC – Liquid Water Content

MVD – Median Volume Diameter

NASA – National Aeronautics and Space Administration

NRC – National Research Council Canada

SAT – Static Air Temperature

SEA – Science Engineering & Associates

TAS – True Air Speed

TWC – Total Water Content

WC – Water Content

Abstract

The Science Engineering and Associates (SEA) Ice Crystal Detector (ICD) is an aircraft mounted hot-wire probe used to measure the bulk water content of clouds. The probe uses two wires, in concave and convex elements, which are heated to a constant temperature and evaporate cloud hydrometeors on contact. Generally, these wires are heated to 140°C and the impact of other temperature settings has not previously been investigated. This work reports on tests performed at the National Research Council's Altitude Icing Wind Tunnel in order to investigate how the probe measurements differ when the wire set temperature is varied from 20°C to 160°C, depending on the ambient conditions. It was found that the probe is able to operate with wire temperatures ranging from 80°C to 160°C. However, the calculated power loss due to convection must be modified in order to account for the temperature of the deicing heater on the probe. Since the deicing element is larger than the hot-wires, it requires more time to heat up to its set temperature of 50°C, which was not considered in this study. It is recommended that measurements with the ICD include a plan to mitigate the impact of the deicing element.

1. Introduction

Hot-wire probes are widely used instruments for measuring the bulk water content of clouds (e.g. [1]– [4]). Hot-wire probes have a simple principle of operation; heated wires are exposed to the environment and make contact with cloud hydrometeors. The hydrometeors are heated up and evaporated leading to power loss across the wires. Some widely used hot-wire probes include the King probe [5], the Nevzorov probe [6], the Robust probe [7] and the Multiwire probe [8]. The operating temperature of hot-wire probes does not need to be above 100°C. Early studies into hot-wire probes suggested that the optimal temperature may be below this threshold. For example, King et al. [5] recommended a temperature between 80°C and 90°C as being ideal for a hot-wire probe and Korolev et al. [6] used 90°C as the operating temperature for the Nevzorov probe. Today, however, as recommended in the user manual, the SEA Ice

Crystal Detector (ICD) probe [9] used on the National Research Council (NRC) Convair 580 research aircraft is operated at a temperature of 140°C and the Nevzorov probe is operated at a temperature of 110°C, both above the 100°C threshold.

From September 2020 to February 2021, several different hot-wire probes were tested at the NRC Altitude Icing Wind Tunnel (AIWT), as reported in [10]. The current report focuses on a subset of those tests performed in February 2021 where the ICD (SN#4005) was tested with varying wire temperatures in order to observe the effect of a changing temperature on the collection efficiency of the probe, a test that had not been done before. The ICD probe has two sensor wires with set temperatures. One wire is a liquid water content (LWC) sensor and the other is a total water content (TWC) sensor. The LWC sensor is convex so ice crystals that make contact will break off and will not be detected, whereas liquid droplets will stick to the sensor and be detected. The TWC sensor is concave, so both liquid water and ice particles will be captured. The probe also has a deicing element, which is held at a constant temperature of 50°C in order to prevent ice buildup on the probe. Sensor wire temperatures were tested at 20°C, 40°C, 80°C, 120°C and 160°C with the LWC and TWC temperature sensors being changed simultaneously [11]. The probe's normal operational temperature is 140°C, and it is typically calibrated by the manufacturer in the range of 80°C to 160°C. For each of these test temperatures, the probe was tested with three sets of AIWT parameters, outlined in Table 1. For each point, 30 seconds of data were collected before droplet spray was turned on in order to observe the dry-air power loss. Reference points were also taken at the normal operational temperature of 140°C along with a Nevzorov probe (SN#300) at its normal operational temperature of 110°C. These reference points use identical pressure, temperature and droplet median volume diameter (MVD) settings and a set true air speed (TAS) of 90 m/s.

Table 1. *Wind tunnel parameter and sensor temperature settings tested throughout this experiment.*

TAS [m/s]	LWC [g/m^3]	MVD [µm]	Static Temperature [°C]	Static Pressure [kPa]	Sensor Temperature [°C]
90	0.5	20	-10	40	20, 40, 80, 120, 160
90	0.5	20	-10	60	20, 40, 80, 120, 160
90	0.5	20	-10	80	20, 40, 80, 120, 160

2. AIWT Facility Description

Hot-wire probes are often tested in wind-tunnels (e.g. [12]). The ICD was tested in the NRC AIWT, a closed-loop wind tunnel capable of simulating flight conditions [13]. The standard section of the wind tunnel is 57cm × 57cm, which allows for air speeds of 5 to 110 m/s.

The air pressure is controlled by evacuating air using a vacuum pump, and can simulate altitudes up to 12.2 km (40 000 ft). A heat exchanger allows for the air temperature in the wind tunnel to be set between -40°C and 30 °C.

The AIWT is capable producing a liquid water spray of 0.1 - 2.5 g/m^3 with droplet MVD between 8 μm and 200 μm [14]. The installation of the ICD in the wind tunnel is shown in Figure 1.

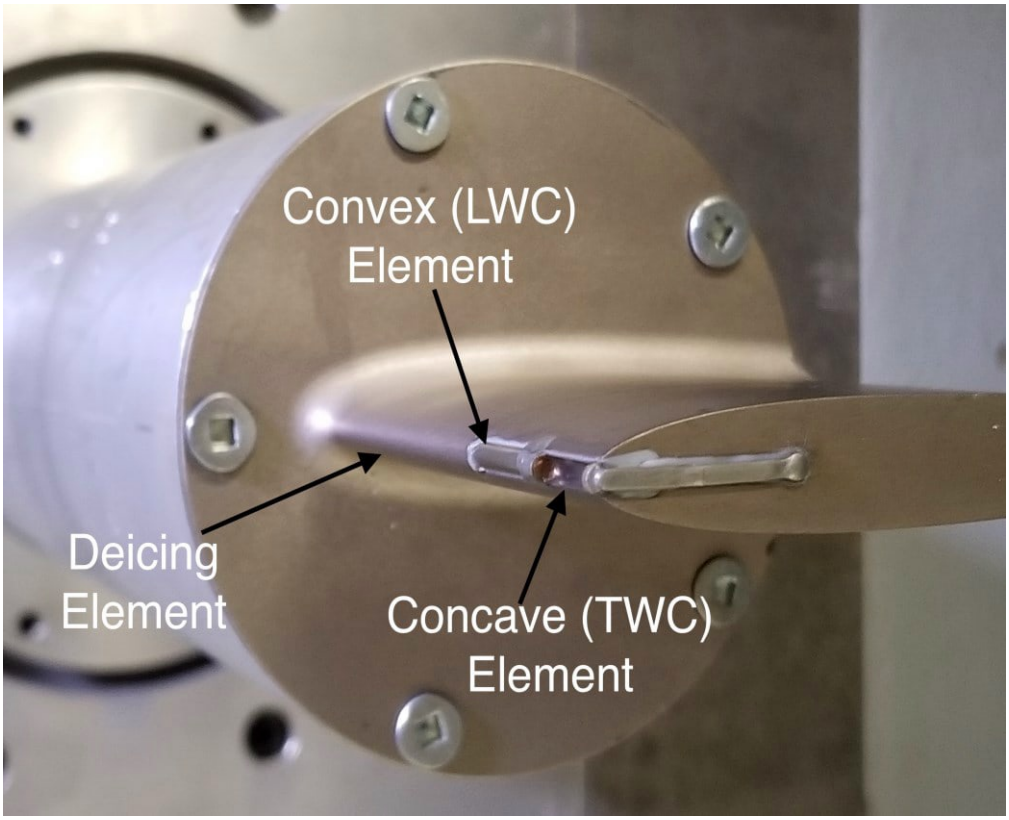

Figure 1. *An image of the ICD probe installation in the AIWT taken from a side window parallel to the ground.*

3. Probe Performance at Low Temperature

When the hot-wire temperatures were set to 20°C, the sensor wires were unable to maintain a constant temperature. Before the water droplet flow was turned on, the wires remained between 30°C and 45°C as reported by the probe's control software. The temperature at these points for the TWC (labeled STWC) and LWC (labeled S083) wires is shown in Figure 2.

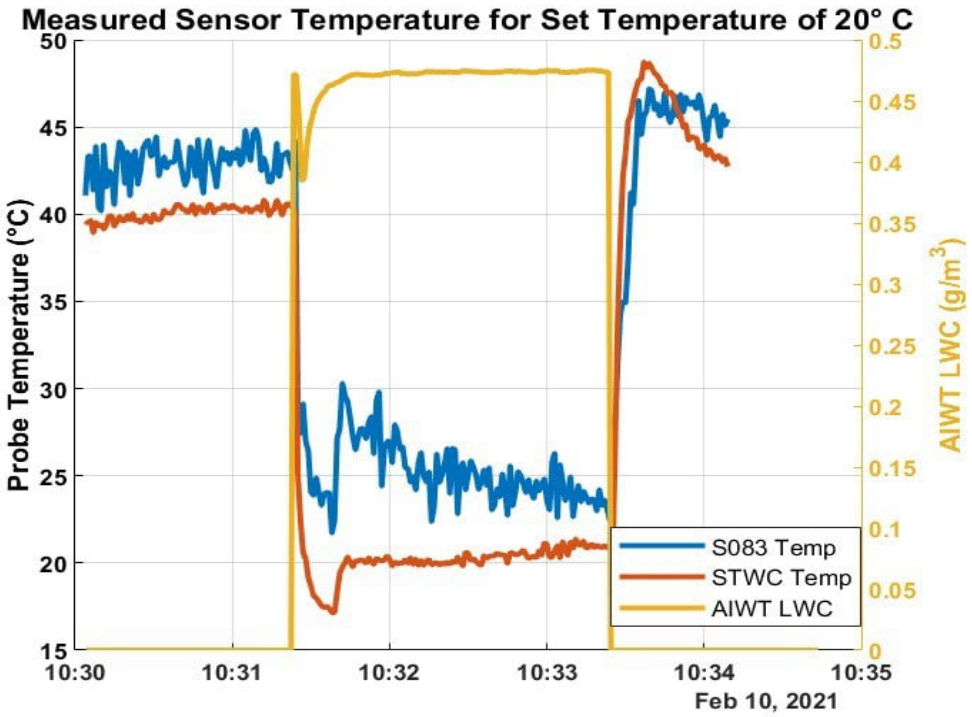

Figure 2. *The time series of the ICD recorded temperature for the LWC and TWC sensors, plotted with the AIWT nominal water content (derived from calibrations with rotating icing cylinder [15]).*

When the droplet flow is turned on, after an adjustment period, the TWC (STWC) temperature holds the desired 20°C in the first two test points and approximately 25°C in the third (not shown). The LWC (S083) temperature signal was very noisy in all test points, but was approximately 25°C. When the flow was turned off, the temperature spiked above the pre-flow temperature.

At this temperature, the LWC sensor did not show any increase in power consumed when the spray was turned on, so there was no clear signal. The signal of the TWC sensor showed a spike in one test point, a small signal in one other, and no signal in the last. The signals detected appear to not be associated with the sensor detecting water, instead they are associated with transient effects from the deicing element discussed in Section 4.1. Due to the lack of clear signal at 20°C, the rest of this report focuses on wire temperatures 40°C and above.

4. Dry Air Power Variation

In normal conditions the dry air power loss can be calculated from the true air speed, the pressure and the ambient temperature [9]. The equation used to calculate the dry air power loss is [16]:

$$P_{dry} = \beta_1 (T_w - SAT) \left(\frac{P_{static} \cdot TAS}{\frac{T_w + SAT}{2} + 273.15K} \right)^{\beta_2} \quad 1$$

where T_w is the sensor wire temperature, SAT is the static air temperature, P_{static} is the static pressure, and TAS is the true air speed. β_1 and β_2 are fitting parameters which are dependent on the geometry of the sensor, and vary between the TWC and LWC elements due to their different shapes. The static pressure, static temperature, and true air speed must be measured externally, meaning that the ICD cannot be used as a standalone sensor. When the wire temperatures were changed, however, Equation 1 did not accurately predict the power loss before or after the test points. So, in order to get any useful data from the plots at varying temperatures it is necessary to modify this equation to better suit the behavior.

4.1. Deicing Temperature Contributions

Since the spray was turned on shortly after the probes, the deicing element of the probe was not allowed enough time to reach the desired value of 50°C. As the deicing element heats up, there is a negative correlation with the wire power for both the LWC and TWC wires particularly for low temperatures, as shown in Figure 3.

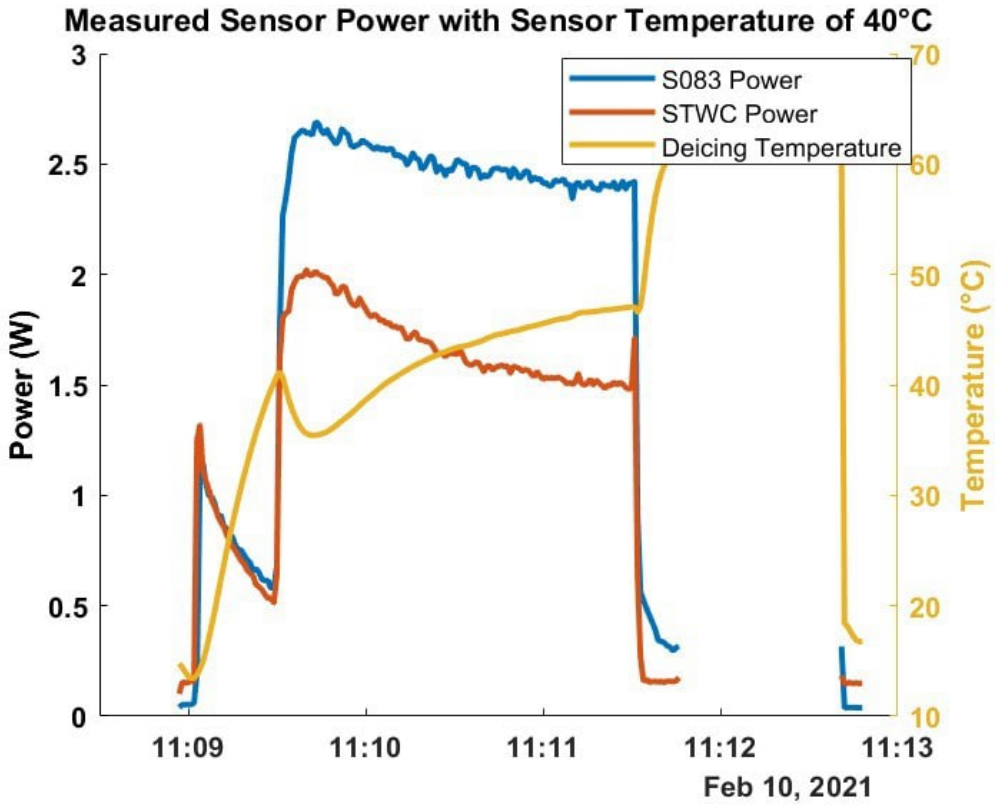

Figure 3. *The time series of the deicing element recorded temperature along with the element power for the STWC and S083 elements.*

This effect causes a decline in power throughout test points which leads to a decrease in measured water content throughout the test point.

Due to the inaccuracy at lower temperature and transient effects of the deicing element, it was necessary to modify the dry-air power loss calculation. An empirical modification to Equation 1 was found, given as Equation 2.

$$P_{dry} = \beta_1 \left(T_w - \frac{SAT + \beta_3 T_{deice}}{2} \right) \left(\frac{P_{static} \cdot TAS}{\frac{T_w + SAT}{2} + 273.15K} \right)^{\beta_2} + \beta_4 (T_w - 140) \qquad 2$$

Equation 2 uses a weighted average of SAT and deicing element temperature T_{deice} when calculating the difference from the wire temperature, which is weighted by the parameter β_3. Equation 2 also adds an intercept term for when the wire temperature deviates from 140°C,

which is weighted by a parameter β_4. Calculated values for the parameters β_1 - β_4 were found using a least-squares optimizer are shown in Table 2.

***Table 2**. Values of $\beta 1$, $\beta 2$, $\beta 3$ and $\beta 4$ for Equation 2 for each sensor found using least squares fit.*

Sensor	**β1**	**β2**	**β3**	**β4**
LWC	0.0067	0.3294	1.1902	0.0066
TWC	0.0093	0.2818	1.2438	0.0047

These changes improve the accuracy of the dry air power loss estimation and reduce the decrease in water content related to the deicing temperature. Figure 4 compares the results of finding the dry air power loss using Equation 2 against a simple offset. Using Equation 2 reduces the correlation between the deicing temperature and calculated WC. The curve observed in the calculated TWC using Equation 2 is still present, but not as extreme as when using a simple offset. There is still bias at low temperatures with an underestimation of the TWC and overestimation of LWC just before the spray is turned on. The TWC is underestimated by 0.07 g/m^3 at 80°C, and 0.04 g/m^3 at 40°C on average. The LWC is overestimated by 0.06 g/m^3 at 40°C on average. This bias indicates that Equation 2 does not entirely capture the probe behavior at these temperatures and should be further improved. The effect of the deicing element temperature is mitigated at higher wire temperatures, since the relative difference between taking the ambient temperature and an average between the ambient and deicing temperature decreases as the wire temperature increases.

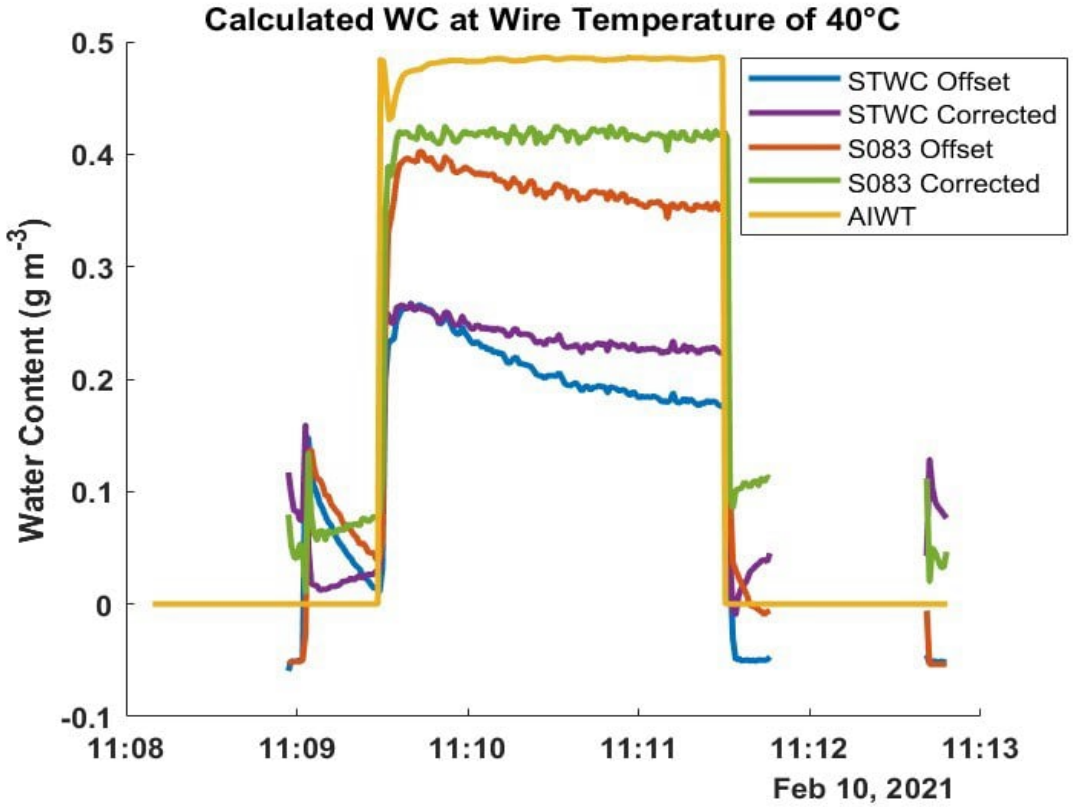

Figure 4*. Water content at a temperature of 40◦C, using the same total power as shown in Figure 3 and two strategies of finding dry air power. The initial strategy used is a simple offset to zero the WC before spray is turned on, the corrected strategy uses Equation 2.*

The effect of the deicing strut may increase the uncertainty of water content measurements in previous wind-tunnel tests, such as [12]. In those tests the dry-air power term does not take the deicing strut into consideration and a correction is applied to zero the out of cloud power just before spray is turned on. If the deicing element had not come to temperature before the spray is turned on, the zeroing applied just before the spray is turned on may bias the water content measurements. Furthermore, since the deicing element temperature shows a drop off when the spray is turned on in Figure 3, not considering the deicing element temperature would increase measurement uncertainty.

5. Changing Wire Temperature

Once the dry air power loss is accounted for, the measured water content for the two probes was calculated. The mean over each of the three test points at each temperature is shown in Figure 5. There are no clear dependencies of the power on the pressure or TAS. At 40°C, the TWC sensor shows a low signal at all three test points, on average 0.19 g/m^3 suggesting only partial evaporation at this temperature. The average calculated water content is equal to the wind tunnel nominal value (0.5 g/m^3) if it is assµed that 35% of the water is being evaporated by the TWC probe at 40°C. However, in the case of partial evaporation on the TWC sensor, 'pooling' would be expected [17], which would lead to extra time taken for water to be expelled after the spray is turned off. As shown in Figure 4, there is no extended signal observed after the spray is turned off, suggesting that there is minimal or no pooling occurring. There is no evidence of significant partial evaporation on the LWC sensor, which may be caused by the geometric differences between the two.

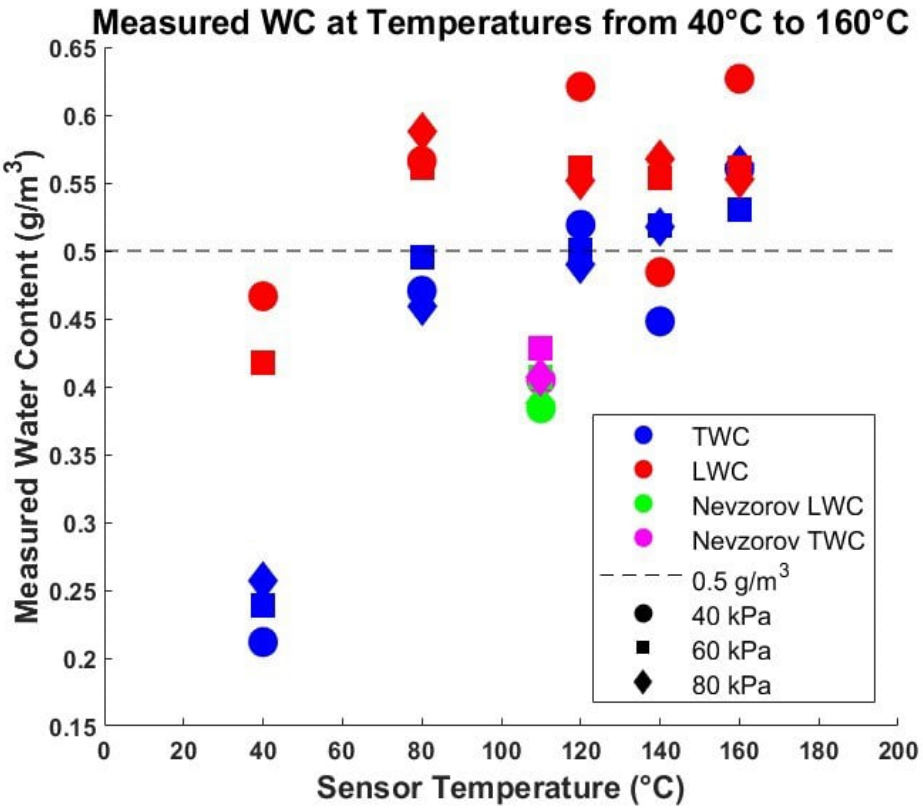

Figure 5. *The measured water content by the ICD TWC (STWC) and LWC (S083) sensors as the temperature varies from 40◦C to 160◦C and the AIWT nominal water content is set to 0.5 g/m³. The color of each point denotes the sensor and the shape denotes the static pressure in the wind tunnel when the measurement was performed.*

From these data, the average water content measured at each temperature was calculated across all pressure values, which is shown in Table 3. At all temperatures, the LWC measurement is higher than the TWC measurement. The measurement difference between sensors above 40◦C is consistent with measurements taken at the standard temperature of 140◦C, droplet sizes below 30 μm and the same wind tunnel nominal value of 0.5 g/m^3 in [16], and are likely caused by the difference in geometry of the sensors.

Table 3. *The measured LWC and TWC for each temperature value, along with reference values from Nevzorov and ICD where the AIWT calibrated WC is held fixed at 0.5 g/m^3.*

Temperature [°C]	LWC [g/m^3]	TWC [g/m^3]
40	0.44 ± 0.06	0.24 ± 0.03
80	0.57 ± 0.01	0.48 ± 0.02
120	0.58 ± 0.05	0.50 ± 0.03
160	0.58 ± 0.04	0.55 ± 0.02

6. Conclusions and Recommendations

These tests gave some clarity on the operational limitations of the ICD and its functioning at set temperatures of 80°C, 120°C and 160°C. The change in power introduced by the deicing element added a challenge in calculations of the dry air power loss. This effect is exaggerated at lower temperatures; however, it is still present at higher temperatures. The strut temperature is an important parameter to characterize in order to avoid measurement bias, since it is not constant in flight. For example, during sharp transitions such as vertical profiling of multi-layer clouds the changing environment may cause to changes in the deicing strut temperature, leading to bias if it is not properly characterized.

The primary concerns of operating a hot-wire probe outside its normal temperature range are pooling at low temperatures and a vapor layer being created at high temperatures [5]. Both of these effects would slow evaporation, but these were not observed in this study. At 40°C, the ICD showed signs of partial evaporation, which limited the WC that was measured. The ICD's measurement of water content was consistent from 80°C to 160°C. Since the effect of the deicing strut temperature variation is more significant at lower temperatures, a higher temperature such as 140°C remains the ideal operational temperature.

In future research, this experiment should be repeated with a few minor adjustments: the temperatures used should be changed, since the probe is unable to sustain a temperature of 20°C, it should be tested at 40°C, 60°C, 80°C, 120°C and 160°C. We also recommend collecting a period of data with the spray and the deicing element both turned off. Without the deicing element turned on, the collector wire temperature should be set to each temperature and approximately 1 minute of clear air data should be collected. These tests should then be repeated at these new temperatures, giving more time, approximately 1.5 minutes, for the deicing strut to reach its set temperature before the spray is turned on. These modifications would provide additional clarity on the impact of the deicing element on the dry air term as well as minimize its effect by allowing it to achieve its set temperature of 50°C before the spray is turned on. The additional temperature of 60°C may also allow for a pattern to be seen with the TWC collector wire's WC measurement, allowing for the partial evaporation seen at 40°C to be better characterized. These findings may also be applicable to other SEA hot-wire sensors of a similar design such as the Robust probe [7] or the multi-wire instrument operation procedure at NASA Glenn Icing Research Tunnel [18].

Acknowledgements

The authors would like to thank the NRC AIWT operators and scientists and the NRC Aeronautical Product Development and Certification (APDC) program that funded this study. We would also like to thank Walter Strapp for his valuable advice and comments.

References

[1] B. Bernstein *et al.*, "The In-Cloud Icing and Large-Drop Experiment Science and Operations Plan," *Leading Edge Atmospherics, LLC*, 2021. https://doi.org/10.21949/1524472

[2] J. R. Minder *et al.*, "P-Type Processes and Predictability: The Winter Precipitation Type Research Multiscale Experiment (WINTRE-MIX)," *Bulletin of the American Meteorological Society*, vol. 104, no. 8, pp. E1469 – E1492, 2023. https://doi.org/10.1175/BAMS-D-22-0095.1

[3] P. Kollias *et al.*, "Experiment of Sea Breeze Convection, Aerosols, Precipitation and Environment (ESCAPE)," *Bulletin of the American Meteorological Society*, 2024. https://doi.org/10.1175/BAMS-D-23-0014.1

[4] D. Baumgardner *et al.*, “Cloud Ice Properties: In Situ Measurement Challenges,” *Meteorological Monographs*, vol. 58, pp. 9.1 – 9.23, 2017. https://doi.org/10.1175/AMSMONOGRAPHS-D-16-0011.1

[5] W. D. King, D. A. Parkin, and R. J. Handsworth, “A Hot-Wire Liquid Water Device Having Fully Calculable Response Characteristics,” *Journal of Applied Meteorology and Climatology*, vol. 17, no. 12, pp. 1809 – 1813,1978. https://doi.org/10.1175/1520-0450(1978)017<1809:AHWLWD>2.0.CO;2

[6] A. V. Korolev *et al.*, “The Nevzorov Airborne Hot-Wire LWC–TWC Probe: Principle of Operation and Performance Characteristics,” *Journal of Atmospheric and Oceanic Technology*, vol. 15, no. 6, pp. 1495 – 1510, 1998. https://doi.org/10.1175/1520-0426(1998)015<1495:TNAHWL>2.0.CO;2

[7] L. Lilie *et al.*: A Multiwire Hot-Wire Device for Measurement of Icing Severity, Total Water Content, Liquid Water Content, and Droplet Diameter. https://arc.aiaa.org/doi/abs/10.2514/6.2005-859 , 2005.

[8] D. L. Rigby, P. M. Struk, and C. S. Bidwell, *Simulation of fluid flow and collection efficiency for an SEA multi-element probe*. https://arc.aiaa.org/doi/abs/10.2514/6.2014-2752

[9] L. Lilie, C. Sivo, and D. Bouley, *Description and Results for a Simple Ice Crystal Detection System for Airborne Applications*, 2016. https://arc.aiaa.org/doi/abs/10.2514/6.2016-4058.

[10] B. M. Esposito *et al.*, “Comparability of Hot-Wire Estimates of Liquid Water Content in SLD Conditions,” June 2023. https://doi.org/10.4271/2023-01-1423.

[11] *Probe Calibration Sheet*, Science Engineering Associates, Inc, 2021.

[12] L. E. Lilie *et al.*, “Test Results for the SEA Ice Crystal Detector (ICD) Under SLD Conditions at the NASA IRT,” 2021.https://doi.org/10.2514/6.2021-2654

[13] D. M. Orchard, C. Clark, and M. Oleskiw, “Development of a supercooled large droplet environment within the NRC Altitude Icing Wind Tunnel,” 2015.

[14] C. Clark and D. Orchard, “Liquid Water Content Instrumentation Study at the NRC AIWT,” Jun 2023. https://doi.org/10.4271/2023-01-1424

[15] C. Clark: “57cm x 57cm Baseline Calibration”, NRC internal technical report, LTR-AL-2021-0018, 2021.

[16] Fleury, Liam, Bliankinshtein, Natalia, Nichman, Leonid, Bala, Kenny, Wolde, Mengistu: “Characterization of NRC Convair-580 hot-wire probes performance using NRC AIWT,” 2023. https://doi.org/10.4224/40003273

[17] Emery E., Miller D., Plaskon S., Strapp W. and Lillie L.: Ice Particle Impact on Cloud Water Content Instrumentation, 42nd AIAA Aerospace Sciences Meeting and Exhibit, 5 - 8 January, 2004, Reno, Nevada US. https://doi.org/10.2514/6.2004-731

[18] L. E. Steen *et al.*, “NASA Glenn Icing Research Tunnel: 2014 and 2015 Cloud Calibration Procedures and Results,” 2015. https://ntrs.nasa.gov/citations/20150009300